ChemPubSoc Europe

DOI: 10.1002/cssc.201200671

Limitations for Current Production in *Geobacter sulfurreducens* Biofilms

P. Sebastian Bonanni,*[a] Dan F. Bradley,[b] Germán D. Schrott,[a] and Juan Pablo Busalmen[a]

Devices that exploit electricity produced by electroactive bacteria such as *Geobacter sulfurreducens* have not yet been demonstrated beyond the laboratory scale. The current densities are far from the maximum that the bacteria can produce because fundamental properties such as the mechanism of extracellular electron transport and factors limiting cell respiration remain unclear. In this work, a strategy for the investigation of electroactive biofilms is presented. Numerical modeling of the response of *G. sulfurreducens* biofilms cultured on a rotating disk electrode has allowed for the discrimination of different limiting steps in the process of current production within a biofilm. The model outputs reveal that extracellular electron transport limits the respiration rate of the cells furthest from the electrode to the extent that cell division is not possible. The mathematical model also demonstrates that recent findings such as the existence of a redox gradient in actively respiring biofilms can be explained by an electron hopping mechanism but not when considering metallic-like conductivities.

Introduction

Geobacter sulfurreducens bacteria can obtain energy by oxidizing organic matter and transferring the resultant electrons to a polarized electrode, generating an electric current. In addition to allowing the use of electrochemical techniques for an accurate analysis of its respiration rate, this ability has opened a broad window for practical applications of these bacteria including treatment of organic wastes with electric current production in microbial fuel cells,[1] microbial electrolysis cells for the synthesis of high-value products,[2] and microbial desalination cells.[3]

Early optimism for high power production using bacteria, based on dramatic progress achieved during the first years of research, has waned.[4] After the improvement of the first experimental fuel-cell design, there has been little advance in increasing the power output.[5] This is largely because of a lack of understanding of the fundamentals behind the current production process; crucial factors such as the electron transport mechanism that allows the conduction of electrons through the biofilm to the electrode and the identification of the limiting step for current production remain under intense discussion.[6]

[a] P. S. Bonanni, G. D. Schrott, Dr. J. P. Busalmen
Lab. de bioelectroquímica, Area de electroquímica y corrosión INTEMA
Juan B. Justo 4302, Mar del Plata (Argentina)
Fax: (+54) 2234810046
E-mail: sebastian.bonanni@fi.mdp.edu.ar

[b] Dr. D. F. Bradley
Department of Chemistry
University of Liverpool
Crown Street, Liverpool L69 7ZD (United Kingdom)

Supporting Information for this article is available on the WWW under http://dx.doi.org/10.1002/cssc.201200671.

Two main mechanisms are currently proposed to explain electron transport from cells to the electrode;[7] electron hopping (superexchange),[6c,h] where electrons are transported through a sequence of redox reactions between cytochromes in the extracellular matrix that connect each cell with the electrode, and metallic-like conduction[6d–f,8] that states that electron transport occurs through conductive filaments that extend from the external membrane of cells into the extracellular environment, connecting cells with cytochromes at the interface that function as an electrochemical gate.[4,7a,9]

Much research has been undertaken to determine which of these mechanisms prevails in the electron transport process, but the results are not yet conclusive. As there is evidence both for and against each mechanism, an intense debate[6a–e,h,10] is taking place. The electron hopping mechanism is based on results from cyclic voltammetry (CV),[11] spectroelectrochemical assays,[6g,11c] and the detection of abundant[12] cytochromes, which are specifically bound to the pili and polysaccharide external matrix[13] that can be reversibly oxidized and reduced by changing the electrode potential[6c,g,9] and can also serve as temporary storage sites for electrons when there is no electron acceptor.[12,14] Conversely, the pili-based mechanism represents a change in paradigm for biological electron transport as it is different from any described mechanism.[6f,10a] It is mainly supported by the high and metallic-like conductivity of pili,[6d,15] which is assumed to be conferred by electronic resonance between aromatic residues,[16] and by pili that are essential for the respiration of iron oxides.[8,17]

Crucial information that will help to determine which of the aforementioned electron transport mechanisms prevails is still lacking.[7b] Although it was demonstrated that the matrix conductivity does not correlate with the abundance of certain external cytochromes,[6d] which was considered an indication of

a lack of cytochrome involvement in the electron-transport mechanism,[6a,10a] the effect on conductivity of the deletion of OmcZ (the only outer membrane cytochrome determined to be essential for current production)[18] is still unknown. Besides, although bioinformatic simulations suggest that charge transfer between assembled pili subunits may be possible[16] the crystallographic structure of pili remains unresolved. Therefore, it is not possible to confirm that aromatic residues in the protein-functional form are separated by distances that allow long-range electron transport through resonance, as required by metallic-like conduction. The spacing between cytochromes associated with pili seems to be larger than that required for an efficient electron transfer between proteins.[10a] The required intermolecular spacing between cytochromes must be demonstrated to validate the electron hopping mechanism. Additionally, as pili were found in cells cultured under lower temperatures (25 °C)[6e,8,15] than those used in most laboratories (30–32 °C),[11a,c,14a,19] the influence of biofilm growing conditions in cytochrome and pili expression should be analyzed. In addition, the analysis of studies that involve genetic mutants is not straightforward; although evidence collected when the gene encoding for the secretion of pili was deleted suggested a role of the protein in the extracellular electron-transport process,[11b,17–18] recent findings revealed that the deletion of that gene also yields a mislocalization of outer membrane cytochromes (OMCs) in the biofilm matrix.[20]

CV and spectroelectrochemical assays show that the transport of electrons through the biofilm exhibits a diffusive behavior[6c,10b,11d] similar to that observed in classical electrochemical systems such as redox hydrogels and film-coated electrodes.[21] In these systems the propagation of electrons is characterized by an apparent diffusion coefficient that follows Fick's laws with the flux proportional to the gradient of reduced compounds in the film.[21c] This concept was recently adapted to explain the electron-transport process in *Geobacter sulfurreducens* biofilms, giving rise to the above mentioned superexchange mechanism. This mechanism proposes that the propagation of electrons occurs because of the existence of a gradient of reduced redox cofactors (most likely OMCs) that mediate the transport from the cells to the electrode.[6c,h,10b] Within *Geobacter* biofilms the OMCs are reduced by respiring cells and at the same time oxidized by the electrode or neighboring OMCs resulting in a concentration gradient where the ratio of oxidized to reduced cofactors decreases with distance from the electrode–biofilm interface.[6c,g] Therefore, cells in close proximity to the electrode surface are in contact with a higher concentration of oxidized cofactor (able to accept the electrons arising from their respiratory chain) than cells closer to the biofilm–solution interface. If the local concentration of oxidized cofactor at the biofilm–solution interface becomes too low to sustain cell duplication and consequently biofilm growth, it may limit the maximum thickness of the biofilms.[6c,g,h] The concentration gradient of the electron donor is expected to be opposite to the one of oxidized OMCs, that is, concentration decreasing towards the electrode.[22] Therefore, with increasing distance from the electrode, the activity of cells in *Geobacter* biofilms is expected to simultaneously decrease because of the lower concentration of local electron acceptors (oxidized OMCs in the matrix) and increase because of a higher concentration of electron donor species.

All of the cells in a biofilm with a film thickness of 50 μm were determined to be metabolically active.[23] According to the model of conduction through pili, this can be explained by the efficient electron transport through the highly conductive[6d,e] filaments in the matrix.[23a] In this case, the potential difference in the biofilm matrix produced by the resistance for electron transport would be minimal and other factors such as pH could limit the metabolic activity of cells.[6e]

Recent experiments[24] have shown the existence of a redox gradient inside the actively respiring biofilm. Additionally, optical sectioning coupled with chronoamperometry revealed that the current produced by the biofilm reaches a limiting value at thicknesses of approximately 40–60 μm with no variation in current even with a subsequent three-fold increase in the biofilm thickness.[24a] This was interpreted as a consequence of cells in the upper layers of the biofilm respiring at a maintenance rate and not contributing to a large extent to the measured current, which suggests that electron transport through the biofilm matrix may not be as efficient as proposed by the model of conduction through pili.

Although studies (including modeling) have been performed to investigate the effect of electron donor concentration[22] and electrode potential[11d,25] on current production, the simultaneous effect of these parameters, which can help to identify the electron transport mechanism that better explains the experimental results, has not been reported. Although the gradient of oxidized cytochromes has been theoretically proposed,[10b] it has not been calculated under real experimental conditions.

In this work, we present a kinetic model that successfully reproduces the response of a *Geobacter sulfurreducens* biofilm grown on a rotating disk electrode (RDE) to variations of electron donor concentration, rate of mass transport to the film, and electrode potential. Current-density calculations were performed based on a Monod-type rate equation that was derived from a recently proposed mechanism,[6h,11b] which relates current production with acetate concentration and the availability of oxidized cytochromes at each layer of the biofilm. The model allows the determination of the limiting step for current production under each of the experimental conditions at different locations with respect to the electrode surface and the solution interface when considering diffusion and convection of the electron donor to the biofilm, diffusion of this species inside the biofilm, reaction between the electron donor and cells, and diffusion of electrons from cells to the electrode. The model also allows the prediction of concentration gradients of both acetate and external oxidized cytochromes and the profile of respiration rate of cells in the biofilm under different operational conditions. In addition, by comparing the output of the model when considering diffusivity of electrons associated with hopping or highly conductive biofilms, the electron transport mechanism that better explains some recent experimental results can be identified.

Results and Discussion

Theory and calculation

The biofilm was represented using a finite element model, with elements distributed for maximum computational efficiency. Each element contained a volume of cells and concentrations of electron donor and oxidized external cytochromes. The steps considered for current production, adapted from the mechanism previously proposed,[6h,11b] were the following:

Step 1: $Ac_{bulk} \xrightarrow{k_{mt}} Ac^*$
Step 2: $Ac^* \xrightarrow{D_{Ac}} Ac_z$
Step 3: $Ac_z + 8\,(Mic_{ox})_z \xrightarrow{k_{ac}} 8\,(Mic_{red})_z + CO_2 + 8\,H^+$
Step 4: $(Mic_{red})_z + (Med_{ox})_z \xrightarrow{k_{omc}} (Mic_{ox})_z + (Med_{red})_z$
Step 5: $(Med_{red})_z \xrightarrow{D_E} (Med_{red})_0$
Step 6: $(Med_{red})_0 \xrightarrow{k_{et}} (Med_{ox})_0 + e^-$

where Ac corresponds to acetate, Med to electron transport mediator in the biofilm matrix, and Mic to *Geobacter* cell.

Step 1 represents the diffusion/convection of acetate (Ac) from the bulk liquid (Ac_{bulk}) to the biofilm–solution interface (Ac*). By using a RDE, the mass transport coefficient (k_{mt}) dependence on the rotation speed can be calculated by using Equation (1):[26]

$$k_{mt} = 0.62\, D_{Ac}{}^{1/3}\, \omega^{1/2}\, \upsilon^{1/6} \tag{1}$$

where D_{Ac} is the diffusivity of acetate in the solution, ω is the rotation speed (radians s^{-1}) and υ is the kinematic viscosity of the solution.

Step 2 represents the diffusion of acetate from the biofilm–solution interface to a distance z from the electrode. The diffusivity of acetate in the biofilm was calculated from that in the solution using a correction factor of 0.8.[22]

Step 3 represents the reaction of acetate with the oxidized cells in layer z $(Mic_{ox})_z$, that produces reduced cells $(Mic_{red})_z$, protons, and carbon dioxide.

Step 4 represents the reaction of reduced cells with an OMC-oxidized mediator in layer z $(Med_{ox})_z$, producing a reduced mediator $(Med_{red})_z$ and regenerating an oxidized cell.

Step 5 is the apparent diffusion of reduced cytochromes from the layer at a distance z to the electrode. Electron transfer between redox centers is affected by several factors including the physical mobility and reactivity of redox-active sites as well as the mobility of counterions.[6g] The complexity of those physical interactions is considered in an apparent diffusion coefficient for electrons (D_E) that relates the concentration gradient of reduced species with the electron flux to the electrode.[6h] The diffusion coefficient can be estimated from CVs performed under acetate depletion conditions.[11e,21c,26]

Step 6 is the heterogeneous electron-transfer reaction between a mediator at the electrode interface $(Med_{red})_0$ and the electrode. The concentration of reduced mediator at the interface is determined by the potential applied to the electrode, according to the Nernst equation.[27]

From steps 3 and 4, a rate equation that relates current production to the amount of oxidized cytochromes and the concentration of electron donor at each position of the biofilm can be obtained [Eq. (2), see the Supporting Information for the detailed derivation]:

$$r_z = \frac{k_1 [Ac]_z [Med_{ox}]_z}{[Ac]_z + K_s [Med_{ox}]_z} \tag{2}$$

where r_z is the acetate consumption rate in the layer at distance z from the electrode [mol m^{-3} s^{-1}], k_1 is the rate constant for current production [s^{-1}], $[Ac]_z$ is acetate concentration in the layer at distance z from the electrode [mol m^{-3}], $[Med_{ox}]_z$ is equal to the concentration of oxidized external cytochromes in the layer at distance z from the electrode [mol m^{-3}], and K_s is the equilibrium constant for cells oxidation (k_{omc}/k_{Ac}).

Equation (2) has the functional form of the Monod equation, which has been used in previous works to account for the variation of current production as a function of acetate concentration[22,25a] and incorporates the dependence of acetate consumption rate on the concentration of oxidized mediator outside of the cell. Therefore, it allows the estimation of the gradients for both acetate and mediator inside the biofilm. If no potential decay is considered, the terms $K_s[Med_{ox}]_z$ and $k_1[Med_{ox}]_z$ are constant throughout the entire biofilm, giving rise to the classical Monod expression.

According to Equation (2), the saturation of cellular activity will depend not only on the concentration of acetate, as predicted by Monod equation, but also on the concentration of oxidized mediators outside the cell. Cell activity can saturate even at low acetate concentrations if the oxidized mediator is not at a concentration sufficiently high to accept electrons at the same rate as acetate oxidation is occurring. Using this equation and including the mass transport processes explained above, the concentration profiles of acetate (electron donor) and oxidized/reduced mediator as well as the current produced by the biofilm were calculated for different operational conditions.

Kinetic parameters k_1 and K_s were estimated by obtaining the values that best fitted the experimental current for different acetate concentrations and electrode potentials at different rotation speeds (Figure 1C, 3B, and Figure S5). The concentration of acetate (electron donor) in the bulk liquid was varied between 0.15 and 13 mM and the effects of the applied potential were analyzed by using a low scan rate CV under turnover conditions.

The apparent diffusivity of electrons inside the biofilm (D_E) was calculated from the CVs of biofilms at increasing scan rates under conditions of depleted electron donor.[11e,21c,26] Under these conditions, only the contribution from reversible electron transfer between the electrode and extracellular cytochromes is assumed to be significant. The concentration of mediator in the biofilm was estimated from the area of the peaks of the CVs,[26] yielding a value close to the value determined by modeling the discharge of biofilms.[12] To avoid limitations on current production produced by the accumulation of protons inside the biofilm,[28] high concentration of buffer

(100 mM) and high rotating speed (500 rpm) were used in the experiments. Under these conditions, there was no increase in current with changing rotation speed or the subsequent addition of buffer, which was considered an indication of the current production not being limited by proton transport inside the biofilm (see the Supporting Information).

Once the kinetic parameters k_1 and K_s were estimated by fitting experimental data, the limitations for current production under different experimental conditions were explored. Because of the similarity between the electrochemical response of this system with that of electroactive biofilms,[6c,h] the strategy used for analyzing electrochemical reactions mediated by redox polymer films[21] was followed.

In each case, the theoretical limiting current (the maximum current value that a given process can sustain) for every process involved in the electron transport mechanism was calculated, at each biofilm layer. The theoretical limiting current for acetate convection to the biofilm (I_A), acetate diffusion inside the biofilm (I_S), reaction rate between cells and acetate (I_k), and apparent electron diffusion from cells to the electrode (I_E) were calculated. To obtain the maximum current that acetate convection to the biofilm can sustain (I_A), it was assumed that there was no acetate at the biofilm–solution interface (i.e., a maximum concentration gradient). Regarding the calculation of the limiting current for acetate diffusion inside the biofilm (I_S), the maximum possible flux from bulk solution to biofilm occurred when the biofilm acetate concentration was zero at the layer of the biofilm being analyzed. The limiting current for reaction kinetics (I_k) considers a uniform concentration of electron donor in the biofilm, equal to that in the bulk solution, and fully oxidized external cytochromes in the layer of the biofilm analyzed. For the apparent electron diffusion, the maximum flux (I_E) is obtained with no oxidized mediator at the layer of the biofilm analyzed. With these considerations Equations (3)–(6) were obtained:

$$I_A = nFk_{mt}[Ac]_{bulk} \tag{3}$$

$$(I_S)_z = 0.8\,nFD_{Ac}\frac{[Ac]_{bulk}}{(Lf - z)} \tag{4}$$

$$(I_K)_z = nF\frac{k_1[Ac]_{bulk}[Med_{ox}]_0}{[Ac]_{bulk} + K_s[Med_{ox}]_0} \tag{5}$$

$$(I_E)_z = FD_E\frac{[Med_{ox}]_0}{z} \tag{6}$$

Under real experimental conditions all processes are operating at the same rate, which determines the current produced by the biofilm. The processes limiting the overall kinetics were identified from the ratio between the operating rate (calculated with the concentrations of electron donor and acceptor determined with the model) and limiting current [Eqs. (7)–(10)].

$$R_A = \frac{[Ac]_{bulk} - [Ac]_{z=Lf}}{[Ac]_{bulk}} \tag{7}$$

$$(R_S)_z = \frac{[Ac]_{bulk} - [Ac]_z}{[Ac]_{bulk}} \tag{8}$$

$$(R_K)_z = \frac{[Ac]_z[Med_{ox}]_z}{[Ac]_z + K_s[Med_{ox}]_z}\frac{[Ac]_{bulk} + K_s[Med_{ox}]_0}{[Ac]_{bulk}[Med_{ox}]_0} \tag{9}$$

$$(R_E)_z = \frac{[Med_{ox}]_0 - [Med_{ox}]_z}{[Med_{ox}]_0} \tag{10}$$

When a ratio is close to one, the corresponding process is operating close to its maximum, thus setting a limit for the production of current.

Modeling of experimental data

The values of the kinetic parameters that best fit the experimental data were $K_s = 2$ and $k_1 = 0.2\ s^{-1}$ ($R^2 = 0.989$ for Figure 1C and $R^2 = 0.996$ for Figure 3B). Using these parameters results obtained with the model were consistent with the current produced by the biofilms under different acetate concentrations (Figure 1C), rotation speeds (Figure S5), and applied potentials (Figure 3B).

The concentration gradients of electron donor and oxidized intermediates for different applied potentials and bulk electron donor concentrations were estimated with the model and compared to estimations considering highly conductive biofilms and recent experimental results.

Concentration gradients of electron donors and oxidized mediators at different bulk electron donor concentrations

The concentration gradient of oxidized mediators and electron donors predicted by the model when considering the diffusivity of electrons (D_E) measured from CVs ($4.8\times10^{-6}\ cm^2\,s^{-1}$, see the Supporting Information) are shown in Figure 1. As mentioned above, redox mediators are at the same time reduced by respiring cells and oxidized by the electrode, which results in a concentration gradient where the ratio of oxidized to reduced form decreases with the distance from the electrode–biofilm interface. The results in Figure 1A show that as the electron donor concentration increases, there is an increasing lack of oxidized mediators that are able to accept electrons in the biofilm, which limits the respiratory activity of the population. Interestingly, mediators on the outermost layers of the biofilm are completely reduced, even when operating at electron donor concentrations as low as 0.5 mM.

Under all of the analyzed concentrations, the electron donor was not depleted inside the biofilm (Figure 1B). As the electron donor concentration in the bulk liquid decreases, the concentration gradient of this species within the biofilm becomes progressively sharper. For example, when the bulk liquid concentration is 13 mM, the concentration inside the biofilm decreases by less than 10% with respect to that in the bulk liquid, whereas at a bulk liquid concentration of 0.15 mM a decrease of almost 45% was estimated. This suggests that the transport of electron donor inside the biofilm may become a limitation for current production when operating at low concentrations.

Direct measurements using confocal Raman microscopy (CRM)[24a] reveal the existence of a potential-dependent[24b]

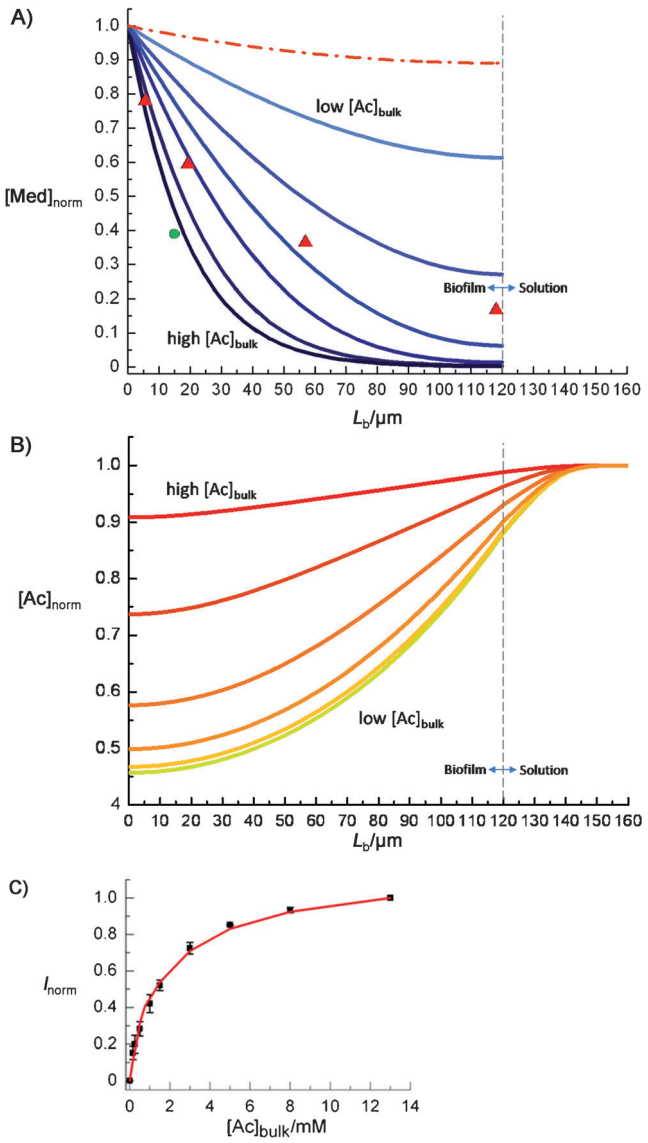

Figure 1. A) Normalized concentration of oxidized mediator in the biofilm ($[Med]_{norm}$), as a function of the distance to the electrode (L_b), predicted by the model for electron hopping with a diffusivity (D_E) of 4.8×10^{-6} $cm^2 s^{-1}$ and bulk acetate concentrations ($[Ac]_{bulk}$) of 0.15, 0.3, 0.5, 1, 3, and 13 mM (——), when considering a conductivity of 1.5 $mS cm^{-1}$ with high acetate concentration and high applied potential (–•–•) and experimental values reported by Snider et al.[24b] (●) and Robuschi et al.[24a] (▲). B) Normalized electron donor concentrations ($[Ac]_{norm}$) for $[Ac]_{bulk}$ = 0.15, 0.3, 0.5, 1, 3, and 13 mM with $D_E = 4.8\times10^{-6}$ $cm^2 s^{-1}$. The concentration of acetate and mediator were normalized by using the values at the bulk liquid and the electrode, respectively. Model parameters: Biofilm thickness L_f = 120 μm, E_{app} = 0.1 V, E_0 = −0.11 V, $[Med]_{tot}$ = 3 mM, K_s = 2, k1 = 0.2 s^{-1}, ω = 700 rpm. C) Normalized current (I_{norm}) as a function of $[Ac]_{bulk}$ (R^2 = 0.989) determined experimentally (■) and modeled with $D_E = 4.8\times10^{-6}$ $cm^2 s^{-1}$(——).

redox gradient inside the biofilm that is produced by the progressive accumulation of reduced species with increasing distance from the electrode. Those findings can be explained when considering the diffusivity of electrons associated with a hopping mechanism, but not by considering metallic-like conductivity attributed to pili (Figure 1 A). The magnitude of the gradient for metallic-like conductivity was determined by considering the apparent diffusion coefficient for electrons ($D_E = 1.3\times10^{-4}$ $cm^2 s^{-1}$) that can be estimated[10a] from a biofilm conductivity of 1.5 $mS cm^{-1}$, which is the value corresponding to a current density produced the biofilm of 7 $A m^{-2}$.[6e] Using this value and according to model estimates, the difference between the fraction of oxidized compounds at the interface and at the outermost biofilm layers is less than 10%, a value that is not in agreement with the recently reported gradients (Figure 1 A). However, when considering the electron diffusivity estimated from CVs related to hopping (4.8×10^{-6} $cm^2 s^{-1}$, see the Supporting Information), the model predicts a sharp redox gradient in the biofilm that agrees with the values obtained experimentally.[24a]

Because of the existence of sharp redox gradients, the respiration rate of cells situated at larger distances from the electrode may be strongly limited by the availability of oxidized mediators.[24a] As shown in Figure 2, model estimations considering electron hopping and high electron donor concentration indicate that cells located beyond 70–80 μm from the electrode might be respiring close to their basal metabolic rate for Fe^{III} respiration (0.7 $mA mg^{-1}$, Esteve-Nuñez, unpublished data). As this rate is not sufficient to allow cell division, it sets a limit for active biofilm thickness. This estimation is supported by experimental results[24a] showing that cells within the first 50 μm

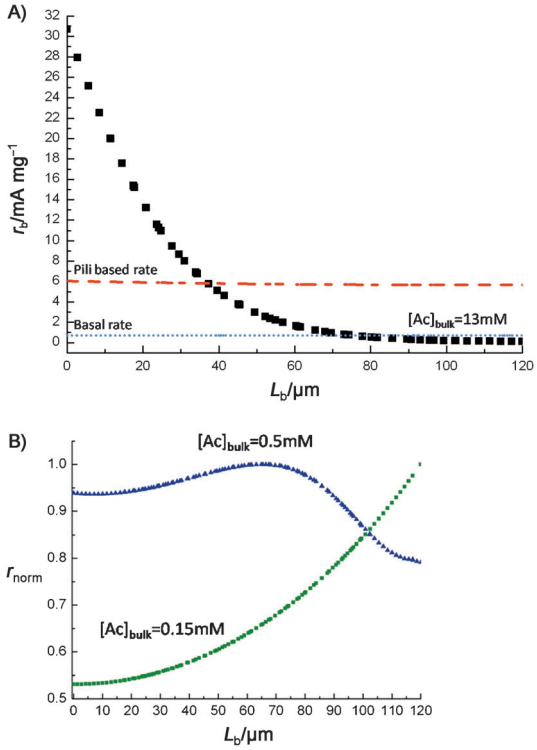

Figure 2. A) Respiration rate of cells (r_b), expressed as current per miligram of protein, as a function of the distance from the electrode (L_b), predicted by the model for electron hopping with a diffusivity of 4.8×10^{-6} $cm^2 s^{-1}$ (■) and estimated considering a conductivity of 1.5 $mS cm^{-1}$(– – –), compared with the basal respiration rate (•••••). Model parameters: $[Ac]_{bulk}$, L_f = 120 μm, E_{app} = 0.100 V, E_0 = −0.11 V, $[Med]_{tot}$ = 3 mM, K_s = 2, k1 = 0.2 s^{-1}, ω = 700 rpm. B) Normalized respiration rates (r_{norm}) predicted by the model for $[Ac]_{bulk}$ = 0.5 mM (▲) and 0.15 mM (■).

from the electrode are metabolically active and likely to be contributing to current production,[23] whereas current becomes independent of biofilm thickness and reaches a stationary value beyond this distance, indicating that the contribution to current production of bacteria located far (>70–80 μm) from the electrode is not significant.[24a]

On the other hand, when considering saturating electron donor and buffer concentrations and the high conductivity values recently reported,[6d] the estimated potential decay across the biofilm estimated with the model is almost negligible. Under these conditions, the model predicts a uniform respiration rate throughout the biofilm (Figure 2) which cannot explain the finite thickness[24a] of the active biofilm that is determined experimentally.

It was recently reported that the current produced by a biofilm increases with its conductivity. This was thought to be because of a relationship between conductivity and the overall internal resistance for electron transport through the biofilm.[6e] Following this reasoning, the maximum distance through which cells can transport electrons, and thus the thickness of the biofilm, is also expected to increase with conductivity. However, biofilms with conductivities differing in orders of magnitude were determined to have almost the same thickness,[6e] suggesting that the measured metallic-like conductivities may not be representative of the pathway used by cells to transport the electrons. Furthermore, the difference between experimental results and model estimations when considering metallic-like conductivities suggests that such pathways may have a lower conductivity. In fact, the conductivity of the electron pathway estimated from CVs in the absence of an electron donor (0.055 mS cm^{-1}, see the Supporting Information) is two orders of magnitude lower than the reported values of biofilm conductivity.

A conductivity of 0.5 mS cm^{-1} or higher is believed to be necessary to explain the response of the biofilm to changes in the applied potential.[25b] Nevertheless, as shown in Figure 3B, the model can account for such results also when considering the diffusivity of electrons estimated from CVs, which is equivalent to a conductivity one order of magnitude lower than that value (for a detailed explanation, see the Supporting Information).

Pili protein is necessary for high current production[11b] and the development of thick biofilms.[11b] It also has a role in surface colonization,[20] cytochrome secretion,[20] and extra-cellular localization.[29] Therefore, it may also play a role in the electron transport process. In the context of the electron hopping mechanism, this role was proposed to be structural,[20,24b] ordering cytochromes in the extracellular network and consequently improving their efficiency as charge carriers. Even though the practical upper limit for reasonably fast electron transfer through proteins was set at 20 Å,[30] the spacing between cytochrome groups anchored to pili was found to be much higher, suggesting that electrons may be transported through pili.[10a] Unfortunately, the spacing of 3.5 Å between aromatic groups, needed for electron transport through pili to occur,[6d] has not been demonstrated.

An alternative mechanism of electron transport from the cells to the electrode may combine cytochromes and pili. In this hypothetical mechanism, when the distances between the cytochromes impede hopping, the electrons may be transported through the aromatic residues of the pili. Alternatively, when distances between aromatic residues impede transport through pili, electrons may be transferred to the surrounding cytochromes. In this case, hopping between cytochromes as well as between cytochromes and pili will be the limiting step of the mechanism, giving rise to the diffusive behavior of the electron transport and to the sharp redox gradient in the biofilm interior experimentally obtained.

Concentration gradients of oxidized mediator for different applied potentials

The concentration gradient of oxidized mediator inside the biofilm changes with the applied potential. The concentration profile of the mediator was obtained for applied potentials covering the complete redox range of *Geobacter* biofilms; the results are shown in Figure 3A. Because of the gating effect of interfacial cytochromes, at potentials below the midpoint of the voltammetric redox signal in Figure 3B (e.g., −0.11 V) the amount of oxidized mediators greatly decreases along the biofilm (Figure 3A), lowering the mean rate of cell respiration and consequently the current produced by the biofilm.

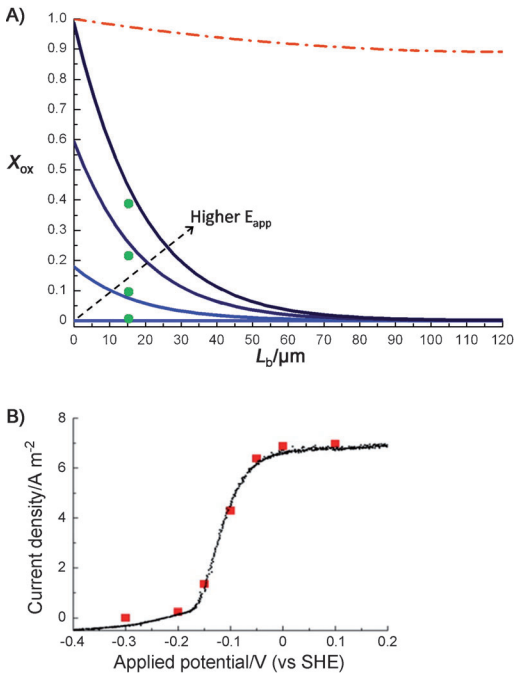

Figure 3. A) Fraction of oxidized mediators (X_{ox}) inside the biofilm as a function of the distance to the electrode (L_b), for $[Ac]_{bulk}$ = 13 mM (high concentration) and applied potentials (E_{app}) of −0.2, −0.04, 0.01, and 0.11 V versus E_0, predicted by the model for electron hopping with a diffusivity of 4.8×10^{-6} cm^2 s^{-1} (——), estimated considering a conductivity of 1.5 mS cm^{-1} and an applied potential of 0.11 V versus E_0 (–•–•) and experimental values reported by Snider et al.[21b] (●). B) Modeled (■) and experimental (···) absolute current density as a function of E_{app} (R^2 = 0.996). Model parameters: $[Ac]_{bulk}$ = 13 mM, L_f = 120 μm, $[Med]_{tot}$ = 3 mM, E_0 = −0.11 V, K_s = 2, k_1 = 0.2 s^{-1}, ω = 700 rpm.

Modeling estimations show that, irrespective of the applied potential, in the upper layers of the biofilm (i.e., at distances greater than 80 μm from the electrode) almost all of the external cytochromes are reduced (Figure 3 A). This is in accordance with recent UV/Vis spectroscopy results that reveal an accumulation of reduced species in the biofilm even under oxidizing potentials[6g] and with CRM results showing that this accumulation is localized in the upper layers of the biofilm.[24a] Furthermore, the fractions of oxidized compounds at 15 μm from the electrode surface, estimated with the model by assuming a diffusivity of $4.8\times10^{-6}\,cm^2\,s^{-1}$, closely agree with those recently measured using interdigitated electrodes under different applied potentials,[24b] demonstrating that such results can be succesfully explained by the electron hopping mechanism. To make this comparison, as the midpoint potential shown in Figure 3 A and the results of the interdigitated electrode experiments are different, the potential of the electrode was expressed against E_0.

According to model estimates, when considering the high conductivity value of $1.5\,mS\,cm^{-1}$, the fractions of oxidized and reduced compounds do not differ to a great extent from the fractions at the electrode interface, irrespective of the applied potential (data not shown). Also, the model predicts no accumulation of reduced compounds at high potentials (Figure 3), demonstrating that such high conductivity is not compatible with the cited UV/Vis spectroscopy results.

Numerical determination of limits for current production

In the following sections, a more extensive analysis of the limitations for current production in the biofilms is performed by determining the ratios given by the limiting process at each layer of the biofilm [Eqs. (7)–(10)] under different experimental conditions, considering electron hopping as the electron transport mechanism. To prevent limitations in current production produced by the accumulation of protons inside the biofilm,[28,31] experiments were performed using high buffer concentrations (100 mM, see the Supporting Information). Limitations to the current production determined by the model are thus restricted to those particular experimental conditions.

Only high applied potentials will be considered in this section. Under these conditions the heterogeneous electron transfer between the biofilm and the electrode was determined to be much faster than the other steps of the mechanism.[11d] Thus, step 6 of the mechanism will be excluded from the analysis.

A process with a ratio equal or close to one is operating at its maximum rate, thus impeding a further increase in current production. Conversely, a ratio close to zero indicates that the corresponding process can work at much faster rates, revealing that such a process is not limiting the current production.

Convection does not limit current production

Acetate is transported from the bulk liquid to the biofilm by convective transport. The rate of mass transport increases with the difference between the bulk liquid and the biofilm–solution interface concentrations and is proportional to a coefficient k_{mt}, which is affected by the electrode rotation speed. An increase in rotation speed improves the mass transport of the electron donor to the biofilm and, thus, increases current production. Protons are a product of cell respiration that negatively affect current production. As they are also transported from the biofilm to the bulk liquid through convection, an increase in rotation speed will also affect current production because of a change in the rate of transport of protons out of the biofilm. The effect of rotation speed in current production was analyzed for different buffer concentrations and the results are shown in Figure S1. Increasing the rotation speed had a great effect on current production at low buffer concentrations, whereas at 100 mM the variation of current was less than 5% (inset of Figure S1 in the Supporting Information). Under these conditions, the only effect of rotation speed on the current is expected to be the modification of mass transport of the electron donor to the biofilm. The negative effect of proton accumulation inside the biofilm[28,31] is avoided because of the high concentration of buffer used in the experiments (see the Supporting Information).

As indicated by the results in Figure S4, the rate of acetate transport to the biofilm through convection is far from its maximum value ($R_A \ll 1$). Therefore, convection does not limit current production in the analyzed range of rotation speeds and bulk acetate concentrations. The current produced by the biofilm increased less than 10% after increasing the rotation speed from 0 to 500 rpm and stabilized at 500 rpm for all of the analyzed acetate concentrations.

High acetate concentration

The results of calculations [using Eqs. (7)–(10)] considering 13 mM acetate are presented in Figure 4 A as a function of the distance from the electrode. Although the nature of the limitation for current production by the biofilm as a whole was determined to be the rate at which cells can metabolize acetate,[12] the limiting step of individual cells depends on their distance from the electrode. According to the model estimations, for distances greater than 60 μm the diffusion of electrons to the electrode is close to its maximum rate (i.e., the ratio is close to 1), reaffirming that the limitation for current production of cells in the upper layers of the biofilm is the rate of electron diffusion to the electrode. At smaller distances from the electrode, as both acetate and oxidized mediators are at high concentrations (Figure 1), current production is limited by the rate at which cells can metabolize the acetate. This rate depends on both acetate intake (step 3 of the mechanism) and transfer of electrons to the intermediates (step 4 of the mechanism).

According to Equation (1), if the limitations for current production introduced by the lack of oxidized intermediates in the upper layers of the biofilm could be avoided, cells throughout the biofilm would respire close to the maximum rate and a current density of approximately $45\,A\,m^{-2}$ would be obtained. This current density is four-times greater than the highest values reported for planar electrodes[32] and, according

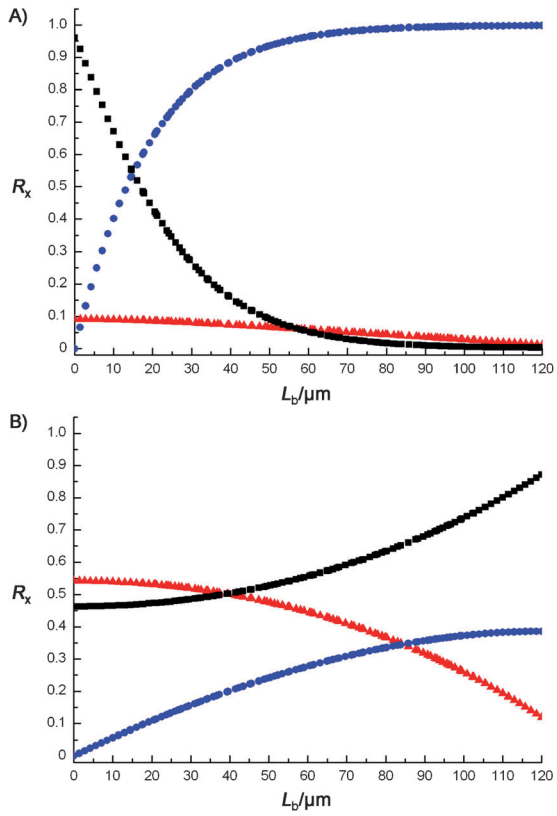

Figure 4. Relative electron flux for (▲) acetate diffusion within the biofilm [R_S, in Eq. (8)]; (■) reaction between cells and the acetate [R_K, in Eq. (9)], and (●) diffusion of electrons from the cells to the electrode [R_E in Eq. (10)] as a function of the distance to the electrode (L_b) considering electron hopping with a diffusivity of 4.8×10^{-6} cm^2 s^{-1} for acetate concentration of A) 13 and B) 0.15 mM. Model parameters: $L_f=120$ μm, $[Med]_{tot}=3$ mM, $K_s=2$, $k_1=0.2$ s^{-1}, $E_0=-0.11$ V, $\omega=700$ rpm, $E_{app}=100$ mV.

to recent estimations, would yield economically sustainable microbial fuel cells and electrolysis cells.[33] Therefore, future efforts should be directed towards reducing the concentration gradient of oxidized redox intermediates in the biofilm.

The transport of electron donors inside the biofilm is operating at rates far from the maximum throughout the biofilm (as indicated by the values of R_s in Figure 4A) and thus is not limiting the current production.

Low acetate concentration

At very low acetate concentrations (0.15 mM) the model predicts that, regardless of the decay in oxidized-mediator concentration, cells respiring at fastest rates are those located near the biofilm–solution interface (Figure 2B) where the acetate concentration is maximal (Figure 1B). The difference in respiration rate is produced by the existence of a sharp gradient of electron donor concentration inside the biofilm (Figure 1B). This indicates that major limitations for cells close to the electrode may be related to the rate of transport of electron donor inside the biofilm.

This was further investigated by calculating R_x [from Eqs. (7)–(9)] for the processes involved in current production (as performed in the previous section) considering a concentration of acetate of 0.15 mM. Results are presented in Figure 4B. The model results show that under these conditions none of the processes are operating at the maximal theoretical rate. As the oxidized cytochromes are not depleted under these conditions (Figure 1A), electron diffusion does not limit current production in any portion of the biofilm (Figure 4B). Acetate diffusion becomes a limiting factor only at small distances from the electrode (<40 μm). As the variation of electron donor concentration has a stronger effect on current at low concentrations (Figure 1C), the current could be greatly increased if the mass transport rate of the electron donor inside the biofilm is enhanced as this would help to equalize the difference between the bulk liquid and the biofilm concentrations.

In the outermost layers of the biofilm, the acetate concentration is similar to that in the bulk liquid (Figure 1B). As oxidized cytochromes are also at a relatively high concentration (Figure 1A), cell respiration in this portion of the biofilm is limited by the rate of acetate metabolization.

Conclusions

The results of a new strategy for the detailed investigation of electroactive biofilms utilizing a combination of hydrodynamic experiments and numerical modeling were presented. A rate expression that considers the effect of electron donor concentration and external oxidized cytochrome availability on current production was derived from a recently proposed mechanism for electron transfer in electroactive biofilms. This expression allowed the simultaneous estimation of the gradients of both the electron donor and electron acceptor species inside the biofilm as well as the detailed kinetic study of the system.

Factors limiting the current production by electroactive cells were dependent on experimental conditions as well as the position of the cells with respect to the electrode surface and solution interface. When using buffer concentrations and rotation speeds under which the accumulation of protons inside the biofilm became negligible, the model revealed that at low acetate concentrations activity of cells close to the electrode was limited by the rate at which acetate diffuses into the biofilm, whereas cells on the outermost layers of the biofilm were determined to be kinetically limited. At high acetate concentrations, the cells furthest from the electrode were limited by the rate at which electrons could be transported through the extra-cellular matrix and were determined to be respiring close to their basal metabolic rate, whereas cells closest to the electrode were limited by the reaction rate between the electron donor and the oxidized cells.

It was demonstrated that the existence of metabolic activity at large distances from the electrode (70–80 μm), the recently reported redox gradient inside the biofilm, and finite thicknesses of the active biofilm can be successfully accounted for by the electron-hopping mechanism of electron transport. It was also shown that neither the redox gradient nor the finite thickness of the active biofilm could be explained when considering metallic-like conductivity. This suggests that, although biofilms are very conductive, the high conductivity may not be repre-

sentative of the pathway used by cells to transport the electrons through the external matrix.

Experimental Section

Biofilms of *Geobacter sulfurreducens* were grown in continuous mode at 32 °C within a 100 cm^3 stirred electrochemical cell. A graphite disk with a diameter of 0.4 cm was used as the working electrode. Before use, the electrode surface was polished with 1000 grade silicon carbide paper and sonicated three times in distilled water. The electrode potential was set at 0.4 V against a standard hydrogen electrode (SHE) with a Ag/AgCl–3 M NaCl reference electrode (RE-6 BASi, IN, USA) and a platinum wire as the counter electrode.

A culture medium lacking electron acceptors and containing sodium bicarbonate solution (100 mM) and acetate (20 mM) as the carbon source was prepared as described in the literature.[34] It was circulated by the electrochemical reactor using PharMed tubing and a low rate peristaltic pump. The pH of the medium was kept constant at a value of 7.3 by bubbling all media reservoirs and the reactor with a mixture of N_2/CO_2 (80:20). The gas mixture was filtered through a Variant C553120 oxygen filter to eliminate oxygen traces. All the electrochemical assays were performed using an Autolab PGSTAT101 potentiostat controlled by Nova 1.6-dedicated software.

The biofilm thickness was estimated by measuring the distance between the air/biofilm and the biofilm/graphite electrode interfaces using a conducting microelectrode controlled by a micromanipulator (Marzhauser Wetzlar—DC-3 K; see the Supporting Information). Biomass accumulation was estimated by the quantification of proteins by using the bicinchoninic acid assay. Biofilm density was calculated from the thickness and biomass data, yielding 10 $mg\,cm^{-3}$. Changes in acetate concentration were achieved by replacing the growth medium with a medium lacking acetate. Aliquots of a concentrated acetate solution were added using a micropipette to obtain the desired working concentration. After approximately 2 h in an acetate-deficient environment, the current produced by the biofilms stabilized at approximately 0.2 $A\,m^{-2}$.This current is thought to be produced from internal pools of electron donors and was independent of rotation speed (data not shown). The rate of mass transport of acetate to the biofilm was changed by varying the rotation speed of the disk electrode from 0 to 700 rpm by using a speed control unit (CTV101 from Radiometer).

The mathematical modeling was performed using Comsol Multiphysics 4.2a software. The model consisted of two mathematical subdomains, one representing the liquid phase and the other representing the biofilm. In the liquid phase acetate is transported by diffusion and convection mechanisms, the rate of the convection was varied by adjusting the rotation speed.[26] In the biofilm subdomain, acetate and electrons were transported by diffusion only. The concentration of the mediator in the biofilm–electrode interface was set by the applied potential according to Nernst equation, taking a half-wave potential of −0.11 V (estimated from the voltammetric response of active biofilms). Equation (2) was used as the rate equation in the biofilm subdomain, considering that 8 mol of intermediate are reduced per mol of acetate consumed. The current was calculated from the integral of the rate equation in the biofilm subdomain.

To test the accuracy of the model output, the oxidation of ferrocyanide was used as a control reaction. The current–density values predicted by the model for different rotation speeds showed a good agreement with experimental values (Figure S3), indicating that convective equations used in the model can accurately describe the dependence of the mass transport rate to the electrode with the rotating speed.

The diffusivity of the electrons in the biofilm was calculated from peak currents of CVs performed at increasing scan rates under non-turnover conditions by linearization to the square root of the scan rate as described in the literature.[26,35] The obtained value (see the Supporting Information) was $4.8\times^{-6}\,cm^2\,s^{-1}$, which is in the order of the values reported for c-type cytochromes in mitochondria,[36] but higher than values obtained for electron diffusion in similar biofilms.[35] This difference can attributed to variations in experimental conditions; in the present work the mass transport rate of counterions, a factor that greatly influences electron-hopping, might have been enhanced by operating at high rotation speeds. The total amount of mediator in the biofilm was estimated from the area of the peaks in CVs, yielding 3 mM. All experiments were performed when the biofilms reached the stationary growth phase, which was approximately 8–9 days after inoculation. Final current densities were in all cases approximately 7 Am^{-2}.

Author Contributions

The experimental work published herein was conducted by P.S.B. and G.D.S. and the numerical simulation by P.S.B. and D.F.B. under the supervision of the latter.

Acknowledgements

The technical assistance of Juan Assarou, Hector Asencio, and José Kochur from INTEMA is greatly acknowledged. The work was supported by the European Union through the BacWire FP7 Collaboration project (contract: NMP4-SL-2009-229337). P.S.B. and G.S. are doctoral fellows from CONICET, Argentina.

Keywords: electron transport · *Geobacter sulfurreducens* · kinetics · mathematical modeling · rotating disk electrode

[1] a) H. Liu, R. Ramnarayanan, B. E. Logan, *Environ. Sci. Technol.* **2004**, *38*, 2281; b) B. Min, J. Kim, S. Oh, J. M. Regan, B. E. Logan, *Water Res.* **2005**, *39*, 4961; c) K. Rabaey, W. Verstraete, *Trends Biotechnol.* **2005**, *23*, 291.
[2] a) R. A. Rozendal, E. Leone, J. Keller, K. Rabaey, *Electrochem. Commun.* **2009**, *11*, 1752; b) K. Rabaey, R. A. Rozendal, *Nat. Rev. Microbiol.* **2010**, *8*, 706; c) H. Liu, S. Grot, B. E. Logan, *Environ. Sci. Technol.* **2005**, *39*, 4317.
[3] X. Cao, X. Huang, P. Liang, K. Xiao, Y. Zhou, X. Zhang, B. E. Logan, *Environ. Sci. Technol.* **2009**, *43*, 7148.
[4] D. R. Lovley, K. P. Nevin, *Curr. Opin. Biotechnol.* **2011**, *22*, 441.
[5] B. E. Logan, *Nat. Rev. Microbiol.* **2009**, *7*, 375.
[6] a) N. S. Malvankar, M. T. Tuominen, D. R. Lovley, *Energy Environ. Sci.* **2012**, *5*, 6247; b) S. M. Strycharz-Glaven, L. M. Tender, *Energy Environ. Sci.* **2012**, *5*, 6250; c) D. R. Bond, S. M. Strycharz, L. Tender, C. I. Torres, *ChemSusChem* **2012**, *5*, 1099; d) N. S. Malvankar, M. Vargas, K. P. Nevin, A. E. Franks, C. Leang, B.-C. Kim, K. Inoue, T. Mester, S. F. Covalla, J. P. Johnson, V. M. Rotello, M. T. Tuominen, D. R. Lovley, *Nat. Nanotechnol.* **2011**, *6*, 573; e) N. S. Malvankar, M. T. Tuominen, D. R. Lovley, *Energy Environ. Sci.* **2012**, *5*, 5790; f) N. S. Malvankar, D. R. Lovley, *ChemSusChem* **2012**, *5*, 1039; g) Y. Liu, D. R. Bond, *ChemSusChem* **2012**, *5*, 1047; h) S. M. Strycharz-Glaven, R. M. Snider, A. Guiseppi-Elie, L. M. Tender, *Energy Environ. Sci.* **2011**, *4*, 4366.
[7] a) D. R. Lovley, T. Ueki, T. Zhang, N. S. Malvankar, P. M. Shrestha, K. A. Flanagan, M. Aklujkar, J. E. Butler, L. Giloteaux, A.-E. Rotaru, D. E. Holmes, A. E. Franks, R. Orellana, C. Risso, K. P. Nevin in *Advances in Microbial*

Physiology, Vol. 59 (Ed.: K. P. Robert), Academic Press, **2011**, pp. 1; b) P. S. Bonanni, G. Schrott, J. P. Busalmen, *Biochem. Soc. Trans.* **2012**, *40*, 1274.
[8] G. Reguera, K. D. McCarthy, T. Mehta, J. S. Nicoll, M. T. Tuominen, D. R. Lovley, *Nature* **2005**, *435*, 1098.
[9] J. P. Busalmen, A. Esteve-Núñez, A. Berná, J. M. Feliu, *Angew. Chem.* **2008**, *120*, 4952; *Angew. Chem. Int. Ed.* **2008**, *47*, 4874.
[10] a) N. S. Malvankar, M. T. Tuominen, D. R. Lovley, *Energy Environ. Sci.* **2012**, *5*, 8651; b) S. M. Strycharz, L. Tender, *ChemSusChem.* **2012**, *5*, 1106.
[11] a) E. Marsili, J. Sun, D. R. Bond, *Electroanalysis* **2010**, *22*, 865; b) H. Richter, K. P. Nevin, H. Jia, D. A. Lowy, D. R. Lovley, L. M. Tender, *Energy Environ. Sci.* **2009**, *2*, 506; c) Y. Liu, H. Kim, R. R. Franklin, D. R. Bond, *ChemPhysChem* **2011**, *12*, 2235; d) S. M. Strycharz, A. P. Malanoski, R. M. Snider, H. Yi, D. R. Lovley, L. M. Tender, *Energy Environ. Sci.* **2011**, *4*, 896; e) K. P. Katuri, S. Rengaraj, P. Kavanagh, V. O'Flaherty, D. Leech, *Langmuir* **2012**, *28*, 7904.
[12] P. S. Bonanni, G. D. Schrott, L. Robuschi, J. P. Busalmen, *Energy Environ. Sci.* **2012**, *5*, 6188.
[13] a) J. B. Rollefson, C. S. Stephen, M. Tien, D. R. Bond, *J. Bacteriol.* **2011**, *193*, 1023; b) K. Inoue, C. Leang, A. E. Franks, T. L. Woodard, K. P. Nevin, D. R. Lovley, *Environ. Microbiol. Rep.* **2011**, *3*, 211; c) K. Inoue, X. Qian, L. Morgado, B.-C. Kim, T. Mester, M. Izallalen, C. A. Salgueiro, D. R. Lovley, *Appl. Environ. Microbiol.* **2010**, *76*, 3999.
[14] a) G. D. Schrott, P. S. Bonanni, L. Robuschi, A. Esteve-Nuñez, J. P. Busalmen, *Electrochim. Acta* **2011**, *56*, 10791; b) N. S. Malvankar, T. Mester, M. T. Tuominen, D. R. Lovley, *ChemPhysChem* **2012**, *13*, 463.
[15] J. P. Veazey, G. Reguera, S. H. Tessmer, *Phys. Rev. E* **2011**, *84*, 060901.
[16] G. T. Feliciano, A. J. R. da Silva, G. Reguera, E. Artacho, *J. Phys. Chem. A* **2012**, *116*, 8023.
[17] G. Reguera, K. P. Nevin, J. S. Nicoll, S. F. Covalla, T. L. Woodard, D. R. Lovley, *Appl. Environ. Microbiol.* **2006**, *72*, 7345.
[18] K. P. Nevin, B.-C. Kim, R. H. Glaven, J. P. Johnson, T. L. Woodard, B. A. Methé, R. J. DiDonato, Jr., S. F. Covalla, A. E. Franks, A. Liu, D. R. Lovley, *PLoS ONE* **2009**, *4*, e5628.
[19] K. Fricke, F. Harnisch, U. Schroder, *Energy Environ. Sci.* **2008**, *1*, 144.
[20] L. V. Richter, S. J. Sandler, R. M. Weis, *J. Bacteriol.* **2012**, *194*, 2551.
[21] a) C. P. Andrieux, J. M. Dumas-Bouchiat, J. M. Savéant, *J. Electroanal. Chem. Interfacial Electrochem.* **1984**, *169*, 9; b) J. Leddy, A. J. Bard, J. T. Maloy, J. M. Savéant, *J. Electroanal. Chem. Interfacial Electrochem.* **1985**, *187*, 205; c) C. P. Andrieux, J. M. Savéant, *J. Electroanal. Chem. Interfacial Electrochem.* **1982**, *142*, 1.
[22] H.-S. Lee, C. s. I. Torres, B. E. Rittmann, *Environ. Sci. Technol.* **2009**, *43*, 7571.
[23] a) A. E. Franks, K. P. Nevin, R. H. Glaven, D. R. Lovley, *ISME J.* **2010**, *4*, 509; b) A. E. Franks, R. H. Glaven, D. R. Lovley, *ChemSusChem* **2012**, *5*, 1092.
[24] a) L. Robuschi, J. P. Tomba, G. D. Schrott, P. S. Bonanni, P. M. Desimone, J. P. Busalmen, *Angew. Chem.* **2013**, *125*, 959; *Angew. Chem. Int. Ed.* **2013**, *52*, 925; b) R. M. Snider, S. M. Strycharz-Glaven, S. D. Tsoi, J. S. Erickson, L. M. Tender, *Proc. Natl. Acad. Sci. USA* **2012**, *109*, 15467.
[25] a) A. Kato Marcus, C. I. Torres, B. E. Rittmann, *Biotechnol. Bioeng.* **2007**, *98*, 1171; b) C. I. Torres, A. K. Marcus, P. Parameswaran, B. E. Rittmann, *Environ. Sci. Technol.* **2008**, *42*, 6593.
[26] A. J. Bard, L. R. Faulkner, *Electrochemical Methods: Fundamentals and Applications, 2nd ed.*, Wiley, New York **2001**.
[27] D. Millo, F. Harnisch, S. A. Patil, H. K. Ly, U. Schröder, P. Hildebrandt, *Angew. Chem.* **2011**, *123*, 2673; *Angew. Chem. Int. Ed.* **2011**, *50*, 2625.
[28] C. I. Torres, A. K. Marcus, B. E. Rittmann, *Biotechnol. Bioeng.* **2008**, *100*, 872.
[29] C. Leang, X. Qian, T. Mester, D. R. Lovley, *Appl. Environ. Microbiol.* **2010**, *76*, 4080.
[30] H. B. Gray, J. R. Winkler, *Proc. Natl. Acad. Sci. USA* **2005**, *102*, 3534.
[31] A. E. Franks, K. P. Nevin, H. Jia, M. Izallalen, T. L. Woodard, D. R. Lovley, *Energy Environ. Sci.* **2009**, *2*, 113.
[32] C. s. I. Torres, R. Krajmalnik-Brown, P. Parameswaran, A. K. Marcus, G. Wanger, Y. A. Gorby, B. E. Rittmann, *Environ. Sci. Technol.* **2009**, *43*, 9519.
[33] T. H. J. A. Sleutels, A. Ter Heijne, C. J. N. Buisman, H. V. M. Hamelers, *ChemSusChem* **2012**, *5*, 1012.
[34] A. Esteve-Nuñez, M. Rothermich, M. Sharma, D. Lovley, *Environ. Microbiol.* **2005**, *7*, 641.
[35] K. P. Katuri, S. Rengaraj, P. Kavanagh, V. O'Flaherty, D. Leech, *Langmuir* **2012**, *28*, 7904.
[36] S. S. Gupte, C. R. Hackenbrock, *J. Biol. Chem.* **1988**, *263*, 5241.

Received: September 7, 2012
Revised: November 15, 2012
Published online on ■■ ■■, 0000

Hop, skip, and jump: A mathematical model that allows the identification of limiting steps for current production under several experimental conditions and in different layers of a biofilm is presented. A comparison of model outputs considering electron hopping and conduction through pili indicates that only electron hopping can account for some recent experimental results.

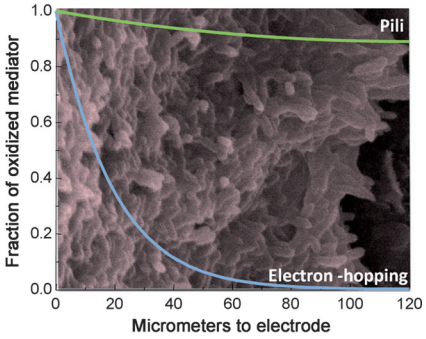

P. S. Bonanni, D. F. Bradley, G. D. Schrott, J. P. Busalmen*

■■ – ■■

Limitations for Current Production in *Geobacter sulfurreducens* Biofilms